

PAPER • OPEN ACCESS

A vibration-based Machine Learning type Structural Health Monitoring methodology for populations of composite aerostructures under uncertainty

To cite this article: I E Saramantas *et al* 2024 *J. Phys.: Conf. Ser.* **2692** 012023

View the [article online](#) for updates and enhancements.



PRIME
PACIFIC RIM MEETING
ON ELECTROCHEMICAL
AND SOLID STATE SCIENCE

HONOLULU, HI
Oct 6–11, 2024

Abstract submission deadline:
April 12, 2024

Learn more and submit!

Joint Meeting of

The Electrochemical Society
•
The Electrochemical Society of Japan
•
Korea Electrochemical Society

A vibration-based Machine Learning type Structural Health Monitoring methodology for populations of composite aerostructures under uncertainty

I E Saramantas¹, P E Spiliotopoulos¹, F T Fera¹, D M Bourdalos¹,
J S Sakellariou¹, S D Fassois¹, Y Ofir², I Kressel², M Tur³,
C Spandonidis⁴

¹Stochastic Mechanical Systems & Automation (SMSA) Laboratory, Dept. of Mechanical Engineering and Aeronautics, University of Patras, 265 04 Patras, Greece

²Advanced Structural Technologies, Dep. 4445, Israel Aerospace Industries (IAI), Engineering Center, Ben-Gurion International Airport, 70 100, Israel

³School of Electrical Engineering, Tel Aviv University, Ramat Aviv 699 78, Israel

⁴PRISMA Electronics S.A., 45 Agias Kyriakis str., P. Faliro, 175 64, Greece

E-mail: ¹jsar@upatras.gr (IES), p.spiliotop@upnet.gr (PES), fationfera@upnet.gr (FTF), dimitrios.bourdalos@upnet.gr (DB), sakj@upatras.gr (JSS), fassois@upatras.gr (SDF), ²yoaofir@iai.co.il (YO), ikressel@iai.co.il (IK), ³tur@tauex.tau.ac.il (MT), ⁴c.spandonidis@prismael.com (CS)

Abstract. A robust to uncertainty Machine Learning (ML) based Structural Health Monitoring methodology for populations of composite aerostructures is postulated. The methodology is founded upon a number of unsupervised ML algorithms for damage detection and a supervised counterpart for damage characterization. Damage detection is specifically based on two types of Healthy Subspace representations: A Multiple Model (MM) and a varying radii Hyper-Sphere (HS) type. Both are built upon response-only vibration acceleration and/or strain signals at properly selected sensor locations. Based on them, Multiple Input Single Output (MISO) Transmittance Function AutoRegressive with eXogenous (TF-ARX) excitation data driven models representing the partial structural dynamics are obtained. Decision making is then based on the model parameter vector that may be transformed and reduced via Principal Component Analysis (PCA). Damage detection is achieved via multi-level information fusion using acceleration and/or strain sensors. Damage characterization, referring to damage type, location, and level determination, is achieved via a hierarchical cosine similarity based algorithm. The methodology is successfully assessed via hundreds of experiments using a population of small-scale composite coupons for the detection and characterization of Delamination and Impact damage under material/manufacturing, temperature, excitation, and experimental uncertainty.

1. Introduction

The dynamics variability/uncertainty in a population of nominally identical composite aerostructures stemming from manufacturing, material uncertainty, as well as varying Environmental and Operating Conditions (EOCs) (such as wind excitation, payload, temperature, assembly/boundary conditions) may be so significant as to mask the effects caused by delicate early-stage damage, as for instance ‘small’ matrix crack, debonding, delamination



and so on. In such cases effective damage diagnosis based on vibration-based Structural Health Monitoring (SHM) methods, which employ the underlying dynamics, may be ineffective if designed as robust in order to properly account for such factors.

The problem of robust SHM for composite aerostructures has been investigated by a number of studies, often under a single uncertainty factor, using, for instance, methods based on Convolutional Neural Networks (CNN), Gaussian Processes (GP), and Principal Component Analysis (PCA) along with either strain [1; 2] or acceleration [3] signals. In a series of studies by some of the present authors, diagnosis of debonding, delamination, and impact-induced damage has been considered for a population of composite aerostructures based on Multiple Model (MM) or Hyper-Sphere (HS) representations of the Healthy Subspace for damage detection and hierarchical characterization employing cosine similarity and either vibration-acceleration [4; 5] or dynamic strain [6; 7] signals. Assessments have been conducted through thousands of test cases employing Monte Carlo simulations with Finite Element (FE) models, as well as experiments involving a population of small-scale composite coupons under manufacturing, temperature, and excitation profile uncertainty.

The *goal* of the present study is to solidify these advances and, based on them, postulate a comprehensive robust Machine Learning (ML) based SHM methodology for populations of composite aerostructures. The methodology makes use of various unsupervised ML algorithms for damage detection, a supervised algorithm for damage characterization, and multi-level information fusion via acceleration and/or strain signals. The methodology is founded upon proper stochastic modeling of the underlying partial structural dynamics through Multiple Input Single Output (MISO) Transmittance Function type AutoRegressive with eXogenous excitation (TF-ARX) data-driven models, and two Healthy Subspace representations: A Multiple Model (MM) and a Hyper-Sphere (HS) based. Decision making is based on the MISO TF-ARX model parameter vector (feature vector) within a corresponding vector space. Once damage is detected, damage hierarchical characterization is achieved via a cosine similarity type algorithm [4; 6]. As indicated, the methodology employs acceleration and/or strain signals along with information fusion at the feature selection and/or decision making levels. Principal Component Analysis (PCA) may be, optionally, used for feature vector dimensionality reduction and potential performance enhancement.

The performance of the postulated methodology is presently assessed with a population of 22 small-scale composite aerostructures under population, experimental, temperature, and excitation uncertainty. Two damage types are considered: Delamination and Impact-induced damage, each of two distinct severity levels (Low/High) implemented in 6 coupons. The performance of the methodology is evaluated in terms of a proper accuracy index using hundreds of evaluation (referred to as Inspection) experiments. It is finally noted that the implementation of the SHM methodology in the form of a prototype system and its assessment on full-scale composite aerostructures is provided in our companion paper [8].

2. The SHM methodology for populations of composite aerostructures under uncertainty

The methodology consists of two operating phases: The Baseline (Training) Phase and the Inspection (Diagnostic) Phase. Its main aspects and available options are described in the sequel, while a flowchart is depicted in Figure 1.

2.1. Step 1: Stochastic Modelling

A partial representation of the structural dynamics, based on each sensor technology, is obtained, using m measured response signals. Of these $m - 1$ act are selected to act as pseudo-inputs and the m -th as output. For each sensor type an n -th order stochastic Transmittance Function Multiple-Input Single-Output (MISO) AutoRegressive with eXogenous excitation TF-ARX

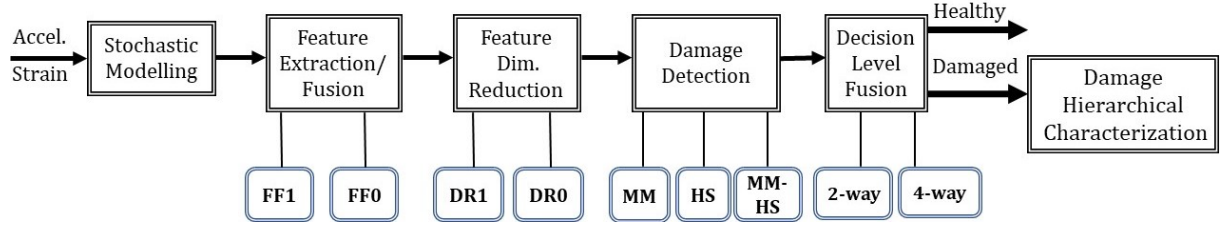


Figure 1: Flowchart of the SHM methodology including its Baseline and Inspection Phases and the available options. Baseline Phase: FF1 if feature fusion is selected (else FF0); DR1 if feature dimensionality reduction is selected (else DR0); Diagnostic algorithm selection as MM, or HS, or both MM-HS. Inspection Phase: Selection of Decision Level Fusion as 2-way using the FF1 option (concatenated feature) and MM or HS, or 4-way using the FF0 option (two types of features) and both MM and HS methods.

model, abbreviated as TF-ARX(n, n), of the following form is employed [4; 6]:

$$y_m[t] + \sum_{i=1}^n a_i \cdot y_m[t-i] = \sum_{j=1}^{m-1} \sum_{i=1}^n b_i^j \cdot y_j[t-i] + w[t] \quad w[t] \sim \text{i.i.d. } \mathcal{N}(0, \sigma_w^2) \quad (1)$$

In the above t designates discrete time, $y_1[t], \dots, y_m[t]$ the measured response signals, $w[t]$ white zero-mean Gaussian noise with variance σ_w^2 , a_i the AR and b_i^j the X parameters ($i \in [1, n]$, $j \in [1, m-1]$), respectively. The model parameter vector $\theta_{st} := [a_1 \dots a_n \ ; \ b_1^1 \dots b_n^1 \ ; \ b_1^{m-1} \dots b_n^{m-1}]^T$ is employed as the feature vector, with $st = s$ indicating the use of strain signals and $st = a$ of their acceleration counterparts. The identification of proper models is based on standard procedures [9]. For damage detection a number of models (and thus corresponding parameter vectors) are obtained for each sensor type using available measurements from a sample of healthy structures from the population under uncertainty. For damage characterization additional models are obtained under each damage type and specific damage scenario (according to damage level and location).

2.2. Step 2: Feature Extraction/Fusion

In this step two options are available to the user: The use of a single sensor type (strain or acceleration - option FF0) or the use of Feature Fusion (option FF1) by concatenating the parameter vectors θ_s and θ_a along with their respective covariance matrices Σ_s and Σ_a , thus leading to a combined parameter vector θ_f and covariance matrix as follows Σ_f [10]:

$$\theta_f := [\theta_s^T \ \theta_a^T]^T \quad \Sigma_f := \begin{bmatrix} \Sigma_s & 0 \\ 0 & \Sigma_a \end{bmatrix}^T \quad (2)$$

2.3. Step 3: Feature Dimensionality Reduction

In this step two options are available to the user: Utilizing (option DR1) or not (option DR0) feature vector(s) dimensionality reduction via Principal Component Analysis (PCA) for potential robustness enhancement. In the former case, the transformed and reduced feature vector(s) are utilized for the construction of the Healthy Subspace.

2.4. Step 4: Diagnosis Methods (selection and implementation)

In this step the damage detection algorithm(s) are selected as either Multiple Model based (option MM) or varying radii Hyper-Sphere based (option HS) or both (option MM-HS). Each

one of the MM and HS options follows distinct approaches in constructing the Healthy Subspace and in making the diagnostic decisions [11; 12]. In the combined approach both are followed. For damage hierarchical characterization a cosine similarity [4; 6] metric is employed within the MM representation framework.

Once the SHM methodology training (Baseline Phase) is complete, diagnostic operation (the Inspection Phase) may initiate once fresh sets of m vibration-response signals per sensor type are available under a currently unknown structural state. For this purpose fresh stochastic models of the same orders and types as those of Step 1 are obtained. Then, damage detection is based on the current parameter (feature) vectors through decision making using the MM and/or HS based detection algorithms (according to the user selections); each one assessing the ‘consistency’ of the current structural state (dynamics) with the ‘Healthy Subspace’ via proper distance metrics [11; 12]. For damage hierarchical characterization a cosine similarity metric is employed and the current stochastic models are classified among those of Step 1 representing the structural dynamics under the types/locations and levels of potential damage.

Decision (for detection and/or characterization) level fusion, in terms of majority voting, may be also selected using multiple diagnostic algorithms and sensor types (according to the user selections). In uncertain (tie) cases, the tie-breaking rule employed favors damage detection.

3. Damage diagnosis for a population of small scale composite aerostructures

The laboratory experiments have been performed at the University of Patras, Greece, using a population of 22 C-shaped composite coupons (Figure 2) characterized by manufacturing/material uncertainty under different Environmental and Operating Conditions (owing to temperature, excitation profile, and experimental setup variability); full details are provided in [5; 7]. The coupons represent part of an actual aerostructure and are made of twelve carbon fiber epoxy resin laminates with $[0/45_2/0/45/0]_S$ ply architecture, with 25×81.8 mm nominal cross-section and 860 mm nominal length. Sixteen coupons are in pristine condition, while six include damage; further details in [5; 7].

Strain and acceleration signals are obtained in each experiment from specific locations on the structure (see Figure 2). In particular, three strain gauges and three accelerometers are placed at corresponding locations for the measurement of longitudinal strain and vertical acceleration signals. Sample mean correction and normalization by the sample standard deviation is performed for each measured signal; details are provided in Table 1. During the experimental procedure each coupon is clamped at its one end via four bolts with a constant torque of 1.6

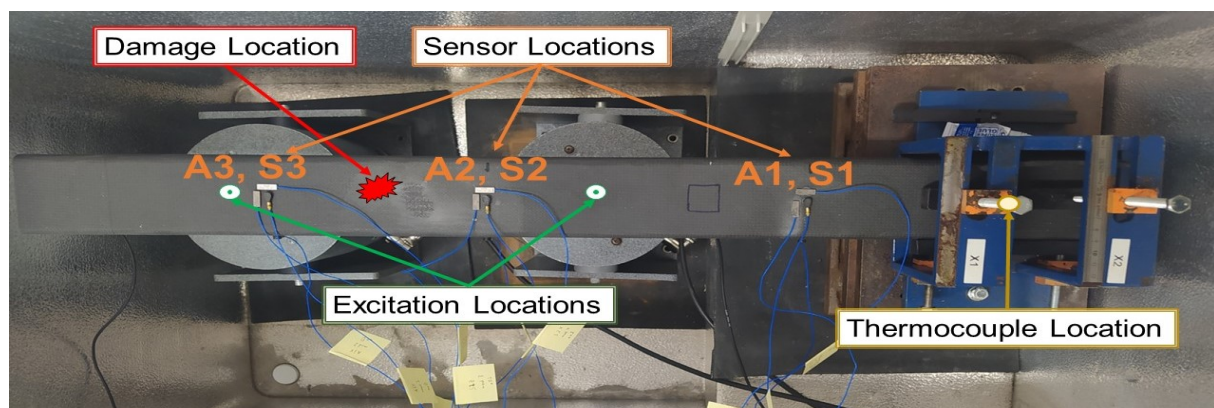


Figure 2: Experimental setup: Photo of the experimental setup with a coupon inside the freezer mounted in the clamping mechanism (right), the locations of excitation, damage and the acceleration (A1, A2, A3) and strain (S1, S2, S3) sensors [5; 7].

Nm, while it is free at the other end. The coupon is excited at two distinct locations with band-limited random force profiles with different spectral characteristics per experiment and location using two electromechanical shakers (Figure 2). The experiments are performed in a freezer under different temperatures in the range of 0–25 °C.

Four damage scenarios are considered: Two levels of rectangular delamination (DL), a low one (DL_L) with delamination area of $20 \times 20 \text{ mm}^2$ and a high one (DL_H) with delamination area $50 \times 50 \text{ mm}^2$, each implemented in a separate coupon with a separation layer of teflon, and two impact-induced (I) damages, a low one (I_L) corresponding to a 13.9 Joule force and a high one (I_H) corresponding to a 23.1 Joule force; details in [5; 7]. All damages are located at 300 mm from the coupon's free end. The effects of the considered damage scenarios on Welch-based MISO-TF magnitude estimates using either acceleration or strain measurements are depicted in Figure 3. Evidently, the effects of damage are almost completely 'masked' by the uncertainty involved in the healthy dynamics. This is indicative of the highly challenging nature of the diagnosis problem tackled.

4. Damage diagnosis results

Damage Detection. 14 healthy coupons are used in the *Baseline Phase* for the training of the SHM methodology, performing 5 experiments per coupon under each of the 6 Baseline temperatures (Table 1) and leading to 420 sets of strain and 420 sets of acceleration signal sets. 420 MISO TF-ARX(100,100) models and an equal number of MISO TF-ARX(90,90) models are obtained from the strain and acceleration signals, respectively (Step 1).

Option FF0 is selected in Step 2, thus using feature vectors exclusively obtained by strain or acceleration signals, as well as option FF1 using feature vector fusion. Dimensionality reduction via PCA is selected for all cases (option DR1) of Step 3, while MM, HS, and MM-HS detection

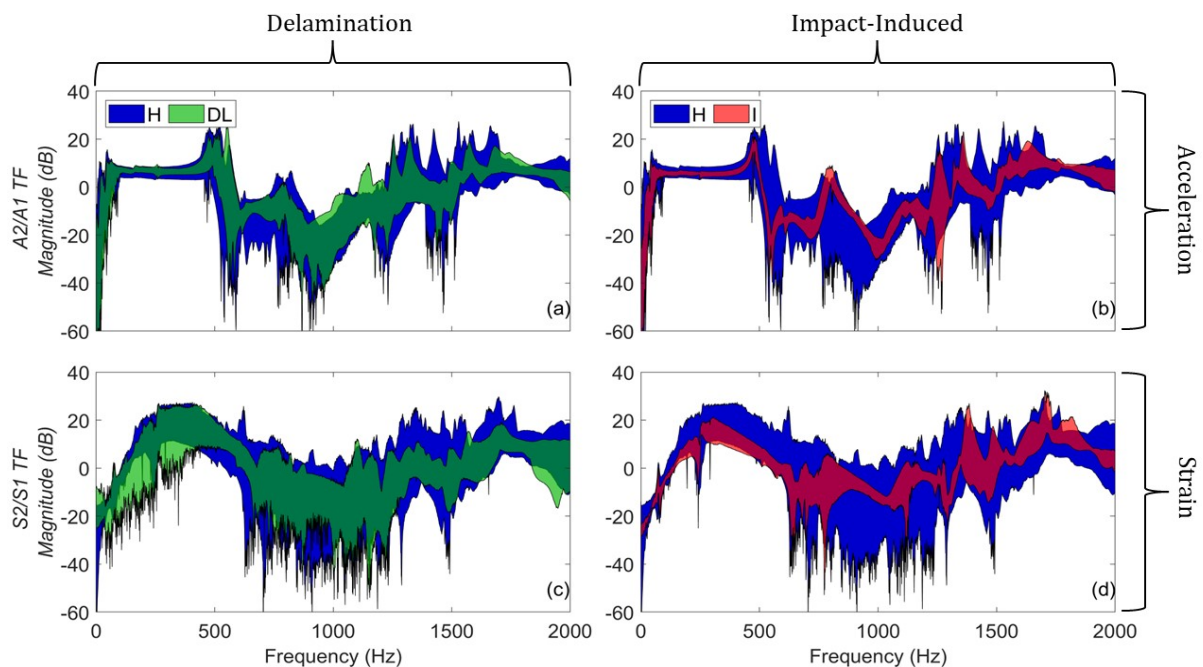


Figure 3: The effects of the considered damage scenarios on Welch-based MISO Transmittance Function magnitude estimates under uncertainty: Delamination damage (left column) and impact-induced damage (right column). Upper row shows A2/A1 acceleration-based estimates, while the lower row shows S2/S1 strain-based estimates [540/120/60 sets of TF magnitude curves under healthy state (blue) /delamination damage (green)/ impact damage (red); see Table 1].

Table 1: Details on the Baseline and Inspection Phases of the SHM methodology.

<i>Structural State</i>	<i>No. of Coupons</i>	<i>Temperatures ($^{\circ}C$)</i>	<i>No. of Expers.</i>
Baseline Phase [Damage Detection]			
Healthy (H)	14	{0, 5, 10, 15, 20, 25}	420*
Inspection Phase [Damage Detection]			
Healthy (H)	2	{1, 2, 3, 4, 6, 7, 8, 9,	120**
Delamination damage (DL)	4	11, 12, 13, 14, 16, 17	240**
Impact-induced damage (I)	2	18, 19, 21, 22, 23, 24}	120**
Baseline Phase [Damage Characterization]			
Delamination damage (DL)	2	{0, 5, 10,	60*
Impact-induced damage (I)	1	15, 20, 25}	30*
Inspection Phase [Damage Characterization]			
Delamination damage (DL)	2	{1, 2, 3, 4, 6, 7, 8, 9, 11, 12, 13, 7	120**
Impact-induced damage (I)	1	14, 16, 118, 19, 21, 22, 23, 24}	60**

*/**: 5/3 experiments per coupon and temperature; Signal details: Sampling $f_s = 4096$ Hz; $N = 81920$ samples (20 s); Signal pre-processing involves sample mean subtraction and normalization by its sample standard deviation.

algorithms are selected in Step 4.

In the *Inspection Phase*, 2 healthy and 6 damaged coupons are used (2 under each delamination DL_L and DL_H , and 1 under each impact-induced damage level I_L and I_H). The SHM methodology's damage detection performance is assessed through 3 experiments per coupon under 20 Inspection temperatures (observe that these are distinct from their Baseline counterparts), resulting in 480 experiments (Table 1). The distance metrics employed by the MM and HS algorithms are based on the Kullback-Leibler divergence and a specific test pseudo-statistic [12], respectively, while the decision-making thresholds are optimally selected based on Receiver Operating Characteristics (ROC) curves. Both 2-way and 4-way decision fusion are selected.

The damage detection and characterization results are presented in terms of accuracy defined as the number of correct decisions divided by the total number of decisions made in the Inspection Phase (correct decision rate). Damage detection results are presented in Figure 4 based on four combinations of the available SHM methodology options: (i) FF1-DR1 including feature fusion and both the MM and HS algorithms (MM-HS) and 2-way decision level fusion, (ii) FF0-DR1 including the MM algorithm and 2-way decision level fusion using strain and acceleration, (iii) FF0-DR1 including the MM-HS option and 2-way decision level fusion based exclusively on acceleration signals, and (iv) FF0-DR1 including MM-HS, 4-way decision level fusion, and both sensor types. Based on the results obtained, the SHM methodology's damage detection performance is excellent in all cases (for any combination of the selected options).

Damage Characterization. 2/1 coupons under delamination/impact-induced damage are employed in the *Baseline Phase*, with 5 experiments per coupon under each of the 6 Baseline temperatures and leading to a total number of 90 experiments (Table 1). Based on these, 60/30 MISO TF-ARX(100,100) models are obtained, representing the partial structural dynamics under Delamination/Impact-induced damage using strain signals and, similarly, 60/30 MISO TF-ARX(90,90) models using acceleration signals. The remaining 120 and 60 experiments (3 experiments per coupon under each of the 20 Inspection temperatures) under Delamination

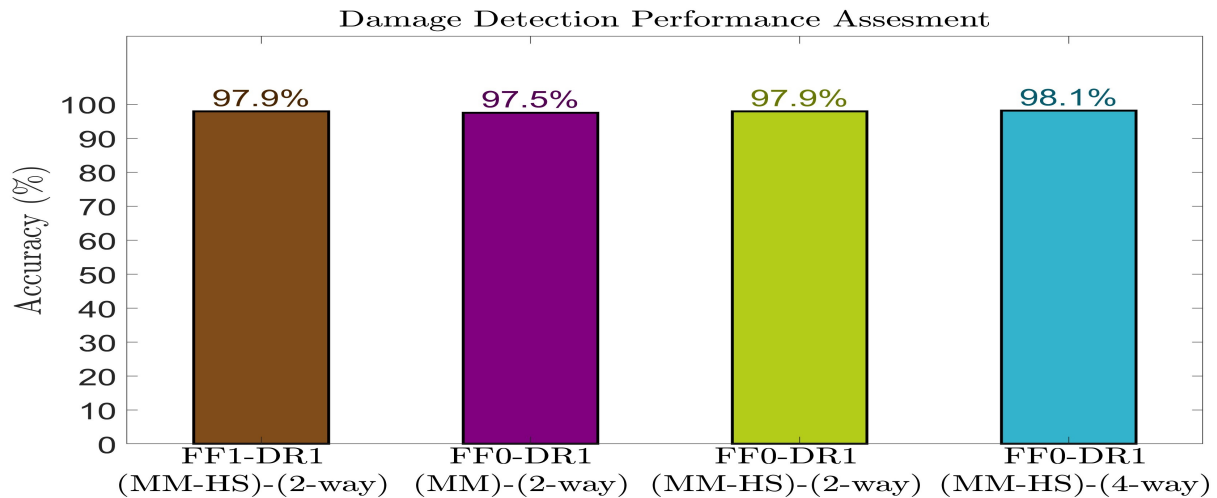


Figure 4: Damage detection results with respect to the selected SHM methodology options: (i) FF1-DR1 using feature fusion both MM and HS methods (MM-HS) and 2-way decision level fusion, (ii) FF0-DR1 using the MM method, 2-way fusion and both sensor technologies, (iii) FF0-DR1 using the MM-HS option, 2-way decision level fusion and acceleration signals, (iv) FF0-DR1 using the MM-HS option, 4-way decision level fusion, both sensor technologies.[120/240/120 experiments under healthy state/delamination damage/impact-induced damage].

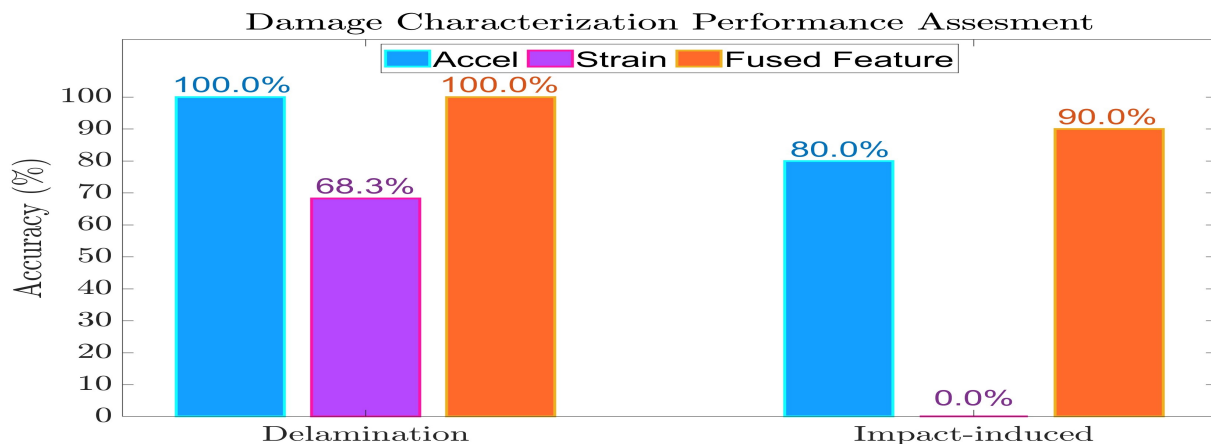


Figure 5: Damage characterization results. Accuracy (%) values using acceleration (blue bars), strain (purple bars) signals and feature vectors fusion (orange bars) (120/60 test cases under delamination/impact-induced damage).

and Impact-induced damage, respectively, are used in the *Inspection Phase* for the SHM methodology' performance assessment in damage characterization.

Damage characterization results are presented in Figure 5. Evidently, Delamination damage is shown to be perfectly characterized using either acceleration signals or both acceleration and strain signals (via feature vector fusion), but the performance achieved is not as high (@ 68.3%) for strain signals. For Impact-induced damage the performance is lower, reaching 80.0% for acceleration signals and 90% for both acceleration and strain signals. Yet, the performance is not acceptable for strain signals; an issue that is under investigation.

5. Concluding remarks

In this study, a Machine Learning based robust Structural Health Monitoring methodology for populations of nominally identical composite aerostructures has been formulated based on strain and/or acceleration signals. The achievable performance has been assessed with hundreds of experiments with Delamination and Impact-induced damages under various uncertainty factors with promising results. Further work is warranted for testing on full-scale structures and further ramifications.

Acknowledgments

The study has been carried out within the framework of the research project ‘Robust to Uncertainty Machine Learning Based Structural Health Monitoring for a Population of Nominally Identical Composite Aerostructures - REALISM’ (project code: T10DIS-00050, MIS 5074648) which is realized within the context of the ‘Bilateral and multilateral R&T cooperation between Greece and Israel’ and is co-financed by the European Regional Development Fund (ERDF) of the European Union and Greek national funds through the Operational Program Competitiveness, Entrepreneurship, and Innovation (EPAnEk).

References

- [1] Lin M, Guo S, He S, Li W and Yang D 2022 *Composite Structures* **286** 115305
- [2] Teimouri H, Milani A, Loeppky J and Seethaler R 2016 *Struct. Health Monit.* **16**(02) 174–184
- [3] Rao A, Lakshmi K and Kumar S 2015 *Adv. Eng. Softw.* **86** 85–106
- [4] Saramantas I E, Konis P E, Kriatsiotis I M, Ofir Y, Kressel I, Spiliotopoulos P E, Fera F, Sakellariou J S, Fassois S D, Giannopoulos F, Spandonidis C, Tur M and Tzioridis Z 2023 *in Proc. of XII Int. Conf. on Structural Dynamics (EURODYN2023)* (Delft, The Netherlands)
- [5] Spiliotopoulos P E, Fera F, Saramantas I E, Ofir Y, Kressel I, Tur M, Konis P E, Kriatsiotis I M, Sakellariou J S, Fassois S D, Giannopoulos F, Spandonidis C and Tzioridis Z 2023 *in Proc. of XII Int. Conf. on Structural Dynamics (EURODYN2023)* (Delft, The Netherlands)
- [6] Fera F T, Saramantas I E, Spiliotopoulos P E, Ofir Y, Kressel I, Fassois S D, Sakellariou J S, Tur M and Spandonidis C 2023 *in Proc. of the X ECCOMAS Thematic Conf. on Smart Struct. and Mat. (SMART2023)* (Patras, Greece)
- [7] Fera F T, Spiliotopoulos P E, Saramantas I E, Ofir Y, Kressel I, Fassois S D, Sakellariou J S, Tur M and Spandonidis C 2023 *in Proc. of the X ECCOMAS Thematic Conf. on Smart Struct. and Mat. (SMART2023)* (Patras, Greece)
- [8] Spiliotopoulos P E, Fera F, Saramantas I E, Sakellariou J S, Fassois S D, Ofir Y, Kressel I, Tur M, Papadopoulos P, Giannopoulos F and Spandonidis C 2023 *in Proc. of VII Int. Conf. of Eng. Against Fail. (ICEAF2023)* (Spetses, Greece)
- [9] Ljung L 1999 *System Identification: Theory for the User, 2nd ed.* (USA: Prentice-Hall, Inc.)
- [10] Thomopoulos S C A 1990 *J. Robotic Syst.* **7** 337–372
- [11] Vamvoudakis-Stefanou K, Sakellariou J and Fassois S 2018 *Mech. Syst. and Sig. Proc.* **111** 149–171
- [12] Vamvoudakis-Stefanou K, Sakellariou J and Fassois S 2022 *Struct. Health Monit.* **21**(2) 465–484